

3-22-2018

Study of Fe₃O₄ nanoparticles degradation process

A. Kozlovskiy

Institute of Nuclear Physics ,Kazakhstan

D. Tuleubayeva

Institute of Nuclear Physics ,Kazakhstan

K. K. Kadyrzhanov

Institute of Nuclear Physics ,Kazakhstan ,

Follow this and additional works at: <https://www.ephys.kz/journal>

 Part of the [Materials Science and Engineering Commons](#), and the [Physics Commons](#)

Recommended Citation

Kozlovskiy, A.; Tuleubayeva, D.; and Kadyrzhanov, K. K. (2018) "Study of Fe₃O₄ nanoparticles degradation process," *Eurasian Journal of Physics and Functional Materials*: Vol. 2: No. 1, Article 6.

DOI: <https://doi.org/10.29317/ejpfm.2018020106>

This Original Study is brought to you for free and open access by Eurasian Journal of Physics and Functional Materials. It has been accepted for inclusion in Eurasian Journal of Physics and Functional Materials by an authorized editor of Eurasian Journal of Physics and Functional Materials.

Study of Fe₃O₄ nanoparticles degradation process

A. Kozlovskiy*, D. Tuleubayeva, K.K. Kadyrzhanov

Institute of Nuclear Physics, Almaty, Kazakhstan

*e-mail: artem88sddt@mail.ru

Received: 16.03.2018

The purpose of this work was to study the oxidation and destruction processes of Fe₃O₄ nanoparticles. As a result, dynamic changes in structure and phase composition of Fe₃O₄ nanoparticles in various pH media was set. The acidity and time dependence of degradation degree on the pH medium was established. It was associated with the appearance of amorphous regions which is due to the presence of hydroxide compounds. By understanding of the nanoparticles degradation rate and degree it becomes possible to clarify the residence time for the nanoparticles, which in turn makes them potential materials for biomedical application. The causes are the high oxygen content and the formation of hydroxide compounds in the structure, as well as subsequent corrosion processes being capable of causing a destruction of the structure.

Keywords: nanostructure, crystal structure, degradation, iron oxide, biomedicine.

Introduction

Production of new structural materials with unique properties is one of the actual problems of the modern technology. In turn, quality of metallic nanostructures depends on the production method, which determines its structural characteristics and physicochemical properties [1-3].

Recently, magnetic nanoparticles, in particular iron oxide (FeO) nanoparticles are of great interest because of their perspective application in making new materials for engineering, ecology and medicine [4-6]. Nanoparticles are biocompatible and can be used in solving various medical problems. Materials based on metal nanoparticles are widely used due to their high specific surface values and the number of surface atoms ratio to the number of the volume atoms in particles. Furthermore, because of the possession of an unusual combination of electrical, magnetic and optical properties that are not characteristic to their bulky counterparts, specific electronic structure of nanoparticles are rather close to the semiconductors [4-7].

The synthesis of Fe-based nanoparticles is very interesting and promising, because of their abundance, relatively low cost as well as new unique properties in the nanoscale. As we know, iron is an essential bio-element and plays an active role in the body as it is an activator of many catalytic processes and participates in the gas transportation in the blood [8-10]. The resistance to oxidation and destruction in media with different acidity, which is determined by the concentration of H⁺ and OH⁻ ions is one of the most important properties of nanoparticles. Hydrogen index (pH) is a value that characterizes the concentration of hydrogen

ions in solutions. For deionized water, from which medical injections are usually prepared, the pH is in the range of 6.5-7, which is typical for a neutral and slightly acidic media, the pH of saline is 5.5 pH and pH of blood is ranged 7.32-7.43.

In this paper, the degradation dynamic of Fe_3O_4 nanoparticles in media with various pH was examined, which determines the period for the nanostructures' applicability and their destruction rate. A detailed analysis of the changes in the structural properties was done. Morphological and structural properties have been studied using scanning electron microscopy, energy dispersive and X-ray diffraction analysis.

Experimental

A mixture of iron chlorides (II), (III) and ammonium hydroxide was used as a starting material for the synthesis of iron oxide nanoparticles. The reaction for the formation of oxide nanoparticles can be presented as below: $\text{FeCl}_2 + 2\text{FeCl}_3 + 8\text{NH}_3 \cdot \text{H}_2\text{O} \rightarrow \text{Fe}_3\text{O}_4 + 8\text{NH}_4\text{Cl} + 4\text{H}_2\text{O}$.

2M of FeCl_2 was dissolved in 2M HCl (1:1) and 1M of FeCl_3 was dissolved in 2M HCl with a molar ratio of 1:2. Then 50 ml NH_4OH (0.7 M) was added after each 5-10 minutes, while stirring by a magnetic stirrer. After the synthesis, the obtained samples were washed in an ultrasound bath and dried at a temperature of 50°C for 24 hours.

The structure and size of the synthesized nanoparticles were studied by using Scanning Electron Microscope (SEM) JEOL JSM-7600F. Energy-dispersive spectrum analysis of nanoparticles was carried out on Scanning Electron Microscope at Hitachi TM3030 and Bruker XFlash MIN SVE, at an accelerating voltage of 15.0 kV, LEI regime. X-ray diffraction analysis was carried out on a D8 ADVANCE ECO diffractometer (Bruker, Germany) using $\text{CuK}\alpha$ radiation. Phase identification and crystal structure studies were performed on Bruker AXSD-IPFRAC.EVA v/4.2 software and the international ICDD PDF-2 database.

In order to study the reactivity, three aqueous solutions with different pH values were chosen: pH1 (strongly acidic medium), pH 5 and pH 7 (neutral acidic medium). The most common chemical reagent used for reducing the high pH of aqueous solutions is HCl. Gradual increase in the concentration of hydrogen ions in the solutions was achieved by using slightly concentrated (0.01M) HCl. The pH rates of solutions were monitored by using a pH meter (Hanna Instruments HI2210-02) within 1 to 10 days.

Results and Discussion

The SEM image presented in Figure 1a shows that the synthesized nanoparticles are spherical. The size dimensions of the samples ranged from 8.64 to 28 nm, with the average diameter of 18.9 nm

From the XRD analysis the following conclusions were made: low-intensity peaks are responsible for X-ray scattering on nanoscale objects, synthesized nanoparticles are polycrystalline Fe_3O_4 (magnetite), with a unit cell parameter of $a=8.34708 \text{ \AA}$, which is different from the reference value. According to the Scherer equation the average crystallinity size was calculated to be 15.93 nm. The crystal lattice parameter was calculated using the Nelson-Taylor extrapolation function:

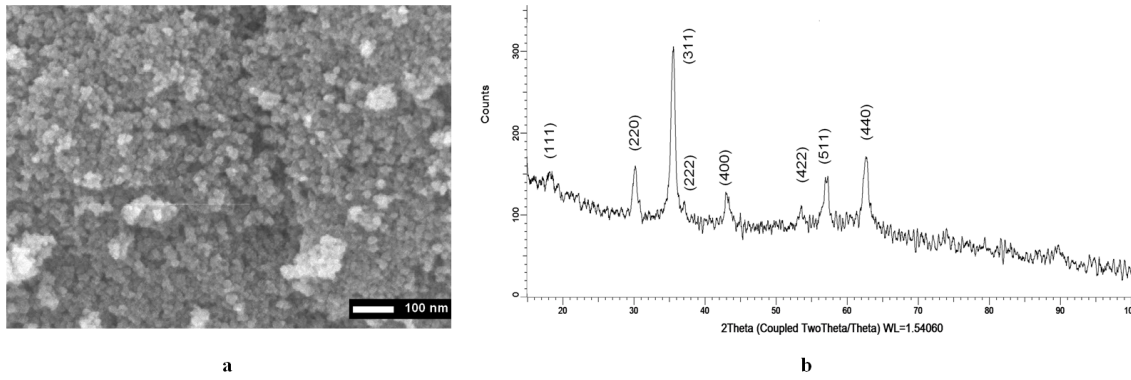


Figure 1. a – SEM image of the iron oxide nanoparticles; b – X-ray diffraction of the nanoparticles.

$$a = f \left[\frac{1}{2} \left(\frac{\cos^2\theta}{\sin\theta} + \frac{\cos\theta}{\theta} \right) \right]. \quad (1)$$

The value and error in determining a parameter were found by linear extrapolation of this function to the zero value of the argument ($\theta = 90^\circ$). Table 1 illustrates the x-ray diffraction data of the sample.

Table 1.

Crystal structure data.

| Phase | hkl | $2\theta^\circ$ | d, Å | L, nm | Cell parameter, Å | FWHM | Crystallinity degree, % | Phase content, % |
|--------------------------------|-----|-----------------|---------|-------|-------------------|-------|-------------------------|------------------|
| Fe ₃ O ₄ | 111 | 18.146 | 4.88486 | 11.30 | a=8.34708 | 0.791 | 73 | 100 |
| | 220 | 30.403 | 2.93763 | 13.81 | | 0.662 | | |
| | 311 | 35.719 | 2.51172 | 13.63 | | 0.680 | | |
| | 222 | 37.237 | 2.41270 | 30.98 | | 0.301 | | |
| | 400 | 43.207 | 2.09234 | 12.95 | | 0.733 | | |
| | 422 | 53.617 | 1.70794 | 16.39 | | 0.603 | | |
| | 511 | 56.980 | 1.61487 | 15.35 | | 0.656 | | |
| | 440 | 62.512 | 1.48459 | 13.03 | | 0.794 | | |

In approximation of lines on the diffractogram the necessary number of symmetric pseudo-Voigt functions, the full width at half maximum (FWHM) was measured. It allowed us characterizing the perfection of the crystal structure and estimating the degree of crystallinity. As a result of the treatment, it was found that the crystallinity degree for the initial sample was 73%. Effect of pH on the crystal structure of Fe₃O₄ nanoparticles was studied by using EDS and XRD methods. The elemental composition dependence of the nanoparticles as a function of the pH media and the retention time in the corresponding solutions are shown in Figure 2.

As it is clear from the graph (Figure 2), there is a sharp increase in the oxygen concentration in an aggressive media, which may be associated with nanoparticles' amorphization. Meanwhile, for neutral media, elemental composition change is insignificant. Furthermore, XRD was used to determine the oxidation and structural change of the nanoparticles. XRD patterns of the samples studied in media with different pH are shown in Figure 3.

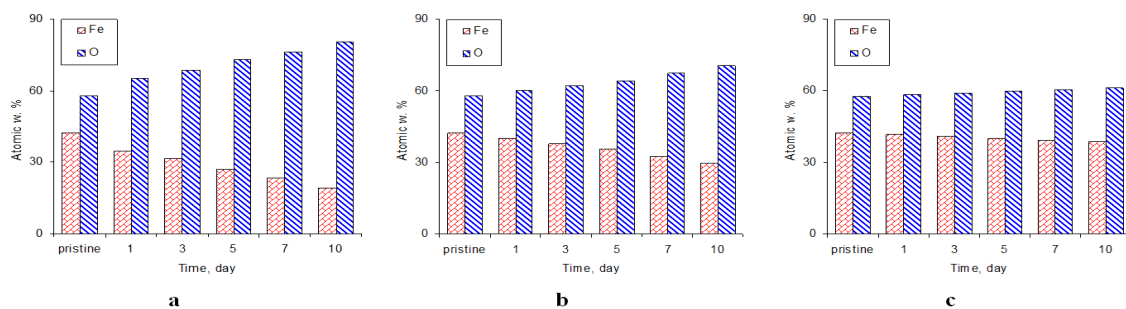


Figure 2. Dependence of iron and oxygen content of the nanoparticles on the residence time in solution with pH= a - 1, b - 5 and c - 7.

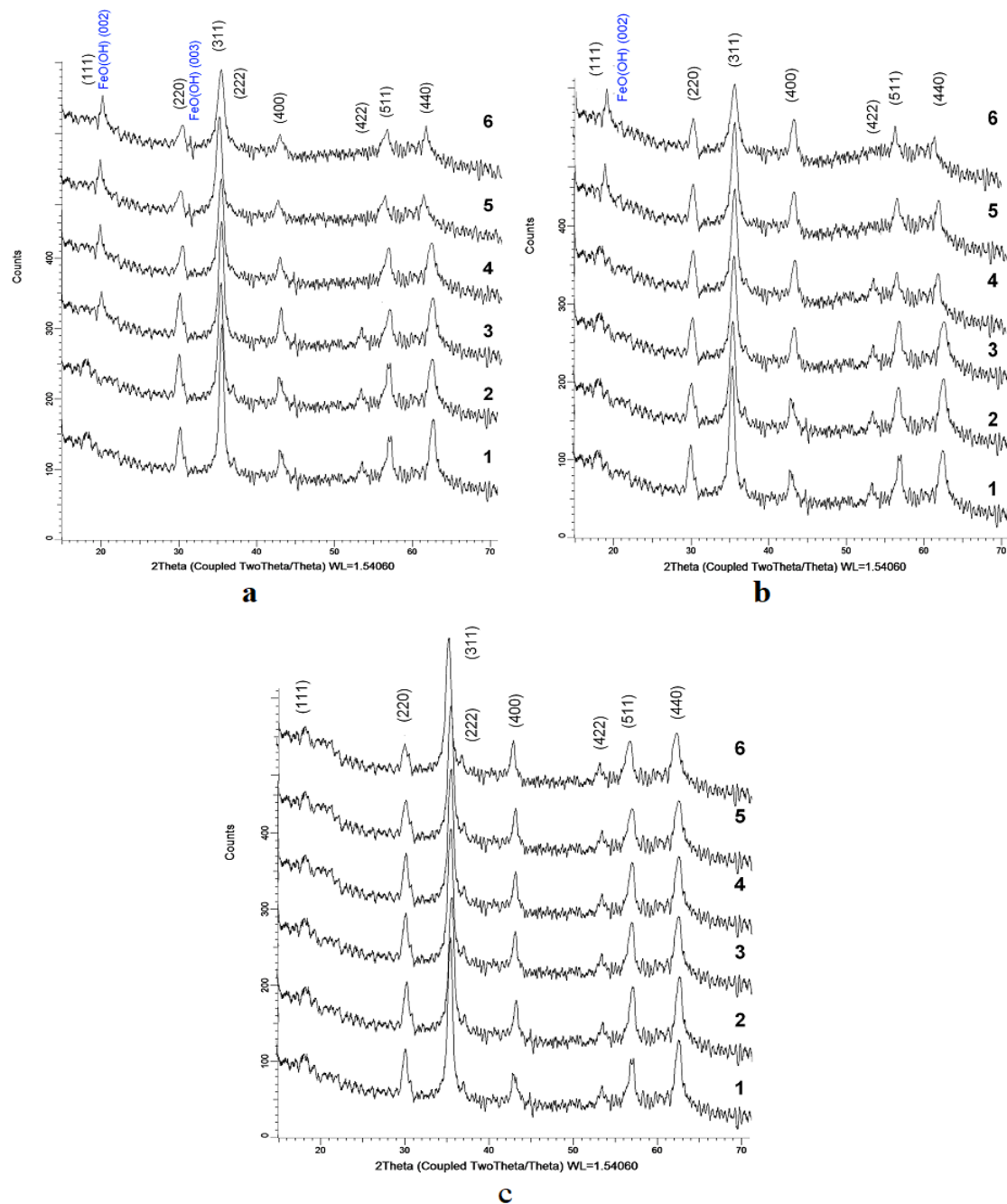


Figure 3. XRD diffractograms of Fe₃O₄ nanoparticles in media with $\bar{d}=1$ (a), $\bar{d}=5$ (b), $\bar{d}=7$ (c): (1) – initial; (2) – 1 day; (3) – 3 days; (4) – 5 days; (5) – 7 days; (6) – 10 days.

From the observed variety of peak intensities and shapes it is assumed that amorphization of the structure and partial degradation of nanoparticles occur in acidic media after 3 days in a medium with pH = 1 and 5. In addition, the broad peaks of hydroxides FeO (OH) were observed in aggressive media on the third day, and for medium with pH = 5 on the fifth day. According to the obtained diffractograms, the Fe₃O₄ peak intensities decreased with the increase of residence time in solutions, while the hydroxide phase of FeO (OH) peaks intensity increased. Based on the peak shape analysis, contribution of various phases in the crystalline structure of nanoparticles during the oxidation process were obtained.

Table 2 present the results of the phase composition assessment.

Table 2.

Quantitative data of the phase composition nanoparticles, %.

| Time | 1 pH | | 5 pH | | 7 pH | |
|---------|--------------------------------|---------|--------------------------------|---------|--------------------------------|---------|
| | Fe ₃ O ₄ | FeO(OH) | Fe ₃ O ₄ | FeO(OH) | Fe ₃ O ₄ | FeO(OH) |
| Initial | 100 | - | 100 | - | 100 | - |
| 1 day | 100 | - | 100 | - | 100 | - |
| 3 days | 96 | 4 | 100 | - | 100 | - |
| 5 days | 91 | 9 | 100 | - | 100 | - |
| 7 days | 85 | 15 | 92 | 8 | 100 | - |
| 10 days | 79 | 21 | 86 | 14 | 100 | - |

As can be seen from the presented data, for nanoparticles being in very acid media, the formation of the hydroxide phase of FeO(OH) begins on third day with oxygen content exceeded 65%, while in neutral media hydroxide phases are not detected. From XRD analysis, we could evaluate the crystallinity degree of obtained nanoparticles, also to trace the dynamic changes of amorphization of the structure in media with different pH. When the lines on the diffractogram were approximated by the necessary number of symmetric pseudo-Voigt functions, the width of registered lines at half their height (FWHM) was measured, which allowed characterizing the perfection of the crystal structure and the degree of crystallinity. The pseudo-Voigt functions used to approximate the profile of X-ray peaks at the diffractogram:

$$PV(x, x_0, \eta, b_L, b_G, A) = A [1(1 - \eta) \times G(x, x_0, b_G) + \eta \times L(x, x_0, b_L)], \quad (2)$$

$$G(x, x_0, b_G) = \exp \left[-\frac{(x - x_0)^2}{2b_G^2} \right], \quad (3)$$

$$L(x, x_0, b_L) = \frac{1}{1 + \left(\frac{x - x_0}{b_L} \right)^2}, \quad (4)$$

where x is the variable corresponding to the reflection angle 2θ ; x_0 specifies the position of function maximum; η is the specific fraction of the Lorentz function; A is a normalizing factor; b_G and b_L are the parameters of Gaussian functions $G(x, x_0, b_G)$ and Lorentz $L(x, x_0, b_L)$. As a criterion for such a correspondence, the root-mean-square deviation can be used, the minimum value of which, with a variation of these parameters, corresponds to their optimal set:

$$\sigma = \sqrt{\frac{\sum_i (PV(x, x_0, \eta, b_L, b_G, A)_i - I_i)^2}{n}}, \quad (5)$$

where is the value of the pseudo-Voigt function, I_i is the value of the experimental intensity, i is the number of the reflex profile point, and n is the number of points in the profile. The results are presented in Table 3.

Table 3.

Data on the crystallinity degree of nanoparticles.

| Time | pH 1 | pH 5 | pH 7 |
|---------|-------|-------|--------|
| Initial | 73±2% | 73±2% | 73±2 % |
| 1 day | 69±3% | 70±3% | 72±3% |
| 3 days | 65±2% | 68±3% | 70±1% |
| 5 days | 54±3% | 65±2% | 68±2% |
| 7 days | 49±4% | 59±3% | 65±2% |
| 10 days | 39±3% | 54±3% | 60±2% |

As it is clear from the table 3 the crystallinity degree of initial sample decreased from 73% to 54% on 5th day and to 39% on 10th day in a medium with a pH=1. This kind of transformation can be seen in a medium with pH=5, where the crystallinity decreases to 65% on 5th day and to 54% on 10th day. It was found that a decrease in the crystallinity degree below 50% leads to a high amorphization degree and partial destruction of the structure due to a large oxygen amount and the formation of hydroxide compound, as well as subsequent corrosion processes capable of causing structural destruction. According to the obtained data, the appearance of hydroxide compound FeO(OH) is characteristic to the decrease of crystallinity degree below 60%. An analysis of the data showed relation between oxide content and nanoparticles amorphization. With the increases oxide content in an acidic medium with pH=1 the degree of texture decreases leading to the nanoparticles amorphization, and in the case of neutral media, the change in the texture coefficients is negligible. From the above data, it can be summarized that a typical iron oxidation occurs. Iron in an acidic medium is oxidized to Fe²⁺. The reactions are presented in Figure 4.

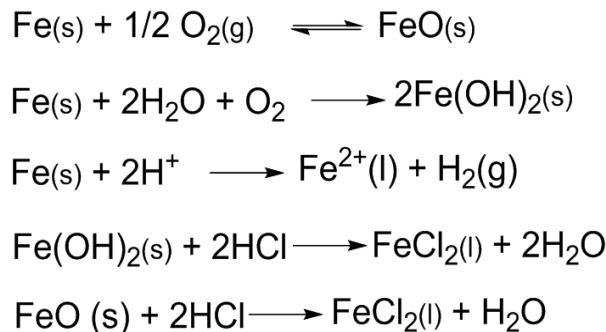


Figure 4. Reactions of Iron Oxidation.

Fe₃O₄ has a spinel structure with formula of Fe₂+Fe₂³⁺O₄²⁻. Allocation of this compound is as following: Fe²⁺ cations and a half of the Fe³⁺ cations occupy octahedral sites, while the other half of the Fe³⁺ cations occupy tetrahedral sites. As a result of the structure degradation, a decrease of Fe³⁺ ions can be

explained with a high concentration and mobility of the H^+ cations at $pH=1$. Consequently a rapid interaction of H^+ ions with Fe_3O_4 and the formation of $FeO(OH)$ with decrease of Fe^{3+} ions occurs. The H^+ cation concentration is very low at $pH=7$, therefore there is no destruction in the crystal structure of Fe_3O_4 . At $pH=5$, an insignificant change of the Fe^{3+} cations is observed.

Conclusions

The change of structural properties and phase composition of nanoparticles Fe_3O_4 in various pH media has been studied. The degradation degree dependence on acidity and residence time in the media has been also studied. This process is associated with the appearance of amorphous regions, which in its turn is due to the appearance of hydroxide compounds. The appearance of amorphous inclusions leads to an increase in the structure deformation, and a decrease in the crystallinity degree below 50% results in a high degree of amorphization of the structure and partial destruction of the structure. The causes are the high oxygen content and the formation of hydroxide compounds in the structure, as well as subsequent corrosion processes being capable of causing a destruction of the structure.

References

- [1] E.Veena Gopalan et al., *Nanoscale Res Lett.* **5** (2010) 889–897.
- [2] L.G. Vivas et al., *Nanotechnology*, **24** (2013) 105703.
- [3] J.Sarkar et al., *Bull. Mater. Sci.* **30** (2007) 271–290.
- [4] S.K. Yen et al., *Theranostics*, **3** (2013) 986–1003.
- [5] M. Safi et al., *ACS Nano.* **5** (2011) 5354–5364.
- [6] M. Eisenstein, *Nat. Methods*, **2** (2005) 484–484.
- [7] R. Asomoza et al., *J. Mater. Sci. Mater. Electron.* **11** (2000) 383.
- [8] S.J. Eichhorn et al., *J Mater Sci.* **45** (2010) 1–33.
- [9] Q.Pankhurst and J. Connolly, *J. Phys. D.* **36** (2003) 167–181.
- [10] S.Mura and J.Nicolas, *P. Nat. Mater.* **12** (2013) 991–1003.